

Dimensional Characterizations of Cosmic Rays Hits on CCD/CMOS sensors with Java Enabled Image Analyzer.

Sherice Malagon-King^{1*}, Olabimtan Olabode. H², Manuel Minino³, Mohammed Aliyu⁴.

^{1,3}10888 Buddy Ellis Rd. 45, Denham Springs, Louisiana 70726, United States of America.

²National Research Institute for Chemical Technology, Department of Industrial and Environmental Pollution, Zaria Kaduna State, Nigeria.

⁴Nigerian Building and Road Research Institute, northwest Zonal Office, Department of Science Laboratory Technology, Kano State, Nigeria.

Corresponding author email: sherice@vent-r.com

Abstract: High energy effects mostly at the upper region of the atmosphere produce falls of lighter particles which degenerate into muons. Muons make up the greater part of the astronomical radiation adrift level, generally electrons, positrons, and photons from sequence occasions. The uniqueness of this radiation keeps attracting interest in its investigations. Hence, in an offer to conceptualize the direct dimensional determination and size classification of cosmic rays, image J software was adopted to statistically explore some specified parameters (area, perimeter, x/horizontal lengths, y/vertical lengths, and roundness) with the hit images by CCD/CMOS image sensors

Keywords: Mouns, cosmic radiation, image J software, CCD/CMOS sensors, and image analysis.

1.0 INTRODUCTION

Astronomical cosmic beam is the word for high magnitude energy radiation that assaults the Earth surface from the intergalactic environment with ultrahigh energies in the scope of 100 - 1000 TeV with the pinnacle of the energy circulation around 0.3 GeV [1]. The force of these astronomical radiation rises with height, demonstrating that it comes from space. It changes with scope, demonstrating that it comprises at any rate halfway of charged particles that are influenced by the ecosphere's attractive field [2]. Enormous beams are high-energy protons and nuclear cores which travel through space at almost the same speed as light. They begin from the sun, from outside of the close planetary system, and from far off the planetary objects. They were sensed by Victor Hess in 1912 in inflatable tests [3]. During the 1920s, the term cosmic beams were instituted by Robert Millikan who made estimations of ionization because of vast beams from profound submerged water level to high elevations around the world. Millikan accepted that his estimations declared that the essential astronomical beams were gamma beams of fiery photons. He further proposed a hypothesis that they were created in interstellar space as side-effects of the combination of hydrogen molecules into the heavier components, and that optional electron was delivered in the climate by Compton dissipating of gamma beams [4]. Yet, at that point, cruising from Java to Netherlands around 1927, Jacob Clay discovered proof, later affirmed in numerous investigations, that enormous beam force increments from the jungles to mid-scopes, which showed that the essential vast beams are avoided by the geomagnetic field and should in this manner be charged particles, not photons [4]. In 1929, Bothe and Kolhörster found charged cosmic beam particles that could infiltrate 4.1 cm of gold. Energetic and charged sub-particles with a high level of energy cannot be induced through photons by Millikan's theory [5]. Direct estimation of enormous beams

(cosmic rays), particularly at lower energies, has gotten conceivable since the dispatch of the primary satellites in the last part of the 1950s [6]. Molecule finders like those utilized in atomic and high-energy material science are utilized on satellites and space tests for an investigation into enormous beams [6]. Upon sway with the Earth's air, cosmic beams can create showers of optional particles that occasionally arrive at the surface. Information from the space telescope by Fermi has been deciphered as proof that a huge portion of essential infinite beams starts from the supernova blasts of stars [6]. Dynamic galactic cores additionally seem to create grandiose beams, because of perceptions of neutrinos and gamma beams from blazar TXS 0506+056 in 2018 [6]. Of essential vast beams, which start outside of Earth's air, about 99% are the cores of notable molecules, and about 1% are single electrons (like beta particles) [6]. Cosmic beams or rays can be isolated into two sorts: galactic cosmic beams and extragalactic cosmic beams which are high-energy particles standing external to the nearby planetary group, and high-energy particles discharged by the sun, essentially in sun-powered emissions [7]. Cosmic beams start as essential grandiose beams, which are those initially delivered in different astrophysical cycles of the cores, about 90% are basic protons, 9% are alpha particles, indistinguishable from helium cores; and 1% are the cores of heavier components, called HZE particles [8]. These portions profoundly cover the energy scope of enormous beams as little division are steady particles of antimatter positrons or antiprotons [9]. Enormous cosmic beams pull in extraordinary premium, because of the harm they exact on microelectronics and life outside the insurance of air and attractive field, and logically because the energies of the most super high-energy cosmic beams have been seen to move toward 3×10^{20} eV around 40 million times the energy of particles quickened by the Large Hadron Collider [10]. One can show that such huge energies may be accomplished by methods for the divergent

component of speeding up in dynamic galactic cores. At 50 J the most noteworthy energy super high-energy cosmic beams have energies tantamount to the active energy of a 90-kilometer-per-hour (56 mph) baseball. Because of these revelations, there has been intriguing in exploring cosmic beams of much more prominent energies [11]. There are two principal classes of identification strategies. The immediate recognition of the essential vast cosmic beams in space or at high heights is by expand borne instruments. Secondly, by the backhanded recognition of auxiliary particles which are broad air showers at higher energies. While there have been recommendations and models for space and inflatable borne identification of air showers, as of now working examinations for high-energy astronomical beams are ground-based. For the most part, direct identification is more exact than roundabout discovery. In any case, the motion of enormous beams diminishes with energy, which hampers direct recognition for the energy range over 1 PeV. Both, immediate and aberrant discovery, is acknowledged by a few methods [12].

Cosmic beam particles, for example, muons and other radiation connect with hardware as they associate particularly with the CCD/CMOS sensor [13]. At the point when muon hits the camera sensor, it associates with camera pixels that are on their way. Because of the picture, we see a light speck or track contingent upon the point to the plane of the sensor. Utilizing picture examination techniques and artificial intelligence we can recognize, measure, arrange, and factually break down the infinite cosmic hits [13]. CCD (charge-coupled gadget) and CMOS (correlative metal-oxide-semiconductor) picture sensors are two distinct advancements for catching pictures carefully. Each has exceptional qualities and shortcomings giving favorable circumstances in various applications. These two kinds of imagers convert light into electric charge and cycle it into

electronic signs. Through the CCD image sensor, each pixel's charge is moved through an extremely set number of yield hubs to be changed over to voltage, cradled, and shipped off-chip as a simple sign. The entirety of the pixels can be committed to light catch, and the yield's consistency is high. With CMOS image device, every pixel possesses its unique charge with voltage change, and the sensor regularly likewise incorporates enhancers, commotion rectification, and digitization connectivity with computerized bits. These different capacities increment the plan unpredictability and decrease the region accessible for a light catch. With every pixel doing its change, consistency is lower, however, it is likewise greatly equal, permitting high absolute data transmission [14]. CCDs and CMOS imagers were both developed in the last part of the 1960s and 1970s by DALSA originator Dr. Savvas Chamberlain. CCD got predominant, essentially with the belief that they gave far unrivaled pictures with the creative innovation accessible. CMOS picture sensors required more consistency and more modest highlights than silicon wafer foundries could convey at that point. Not until the 1990s did lithography create to the point that originators could start presenting a defense for CMOS imagers once more. Reestablished interest in CMOS depended on desires for brought down force utilization, camera-on-a-chip combination, and brought down creation costs from the reuse of standard rationale and memory gadget manufacture. Accomplishing these advantages by and by while at the same time conveying high picture quality has taken undeniably additional time, cash, and cycle variation than unique projections proposed, however, CMOS imagers have joined CCDs as standard, developed innovation [15]. In this unique situation, a java-based image analyzer was integrated into exploiting the dimensions of cosmic hits produces with CMOS/CCD image sensors.

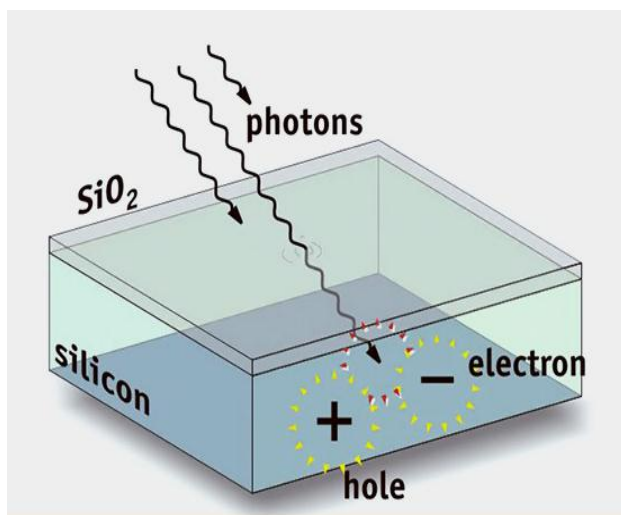


Figure 1. CCD and CMOS imagers both depend on the photoelectric effect to create electrical signal from light [15]

2.0 METHODOLOGY

Four distinct categories of cosmic hits (spot like worm-like, tracks like, and deblending/join track hits) through a charge-coupled device (CCD) and complementary metal-oxide-semiconductor (CMOS) images according to [16], [17], [18], [19] and [20] were technically analyzed with Image J 1.52s java 1.6.0_20 (32-bit) software in estimating their average actual mean areas, distances in terms of the perimeter, horizontal length, vertical length, and circularities.

3.0 RESULTS AND DISCUSSION

Table 1. Image analyzer general scale set up

Property	Value
Distance (pixels)	13.8509
Known distance	1.00
Pixel aspect ratio	1.0
Unit of length	cm
Scale (pixels/cm)	13.8604

Table 2. Image analysis and properties of spot like cosmic hits

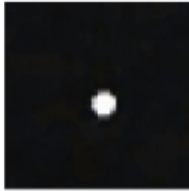
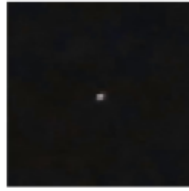

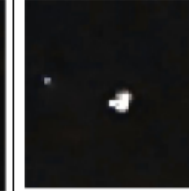
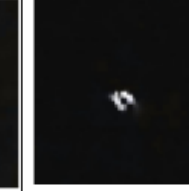
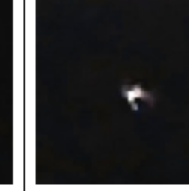




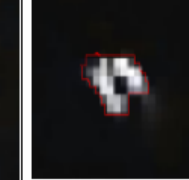

Property	A1	A2	A3	A4	A5	A6
Image format	PNG	PNG	PNG	PNG	PNG	PNG
Magnification (%)	300	297	306	308	314	311
Size (Kilobyte)	193	194	185	190	179	181
Frame (cm)	16.3 X 16.10	15.96 X 16.24	15.67 X 15.74	16.17 X 15.67	15.52 X 15.38	15.52 X 15.52
Frame(pixel)	222 X 223	221 X 225	217 X 218	224 X 217	215 X 213	215 X 215
Original image						
Analyzed image						

Table 3. Image analysis and properties of worm like cosmic hits

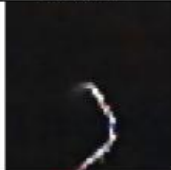
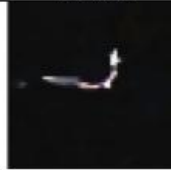
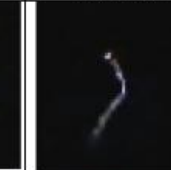
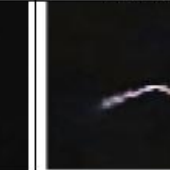


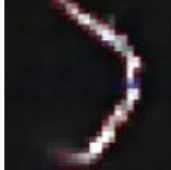



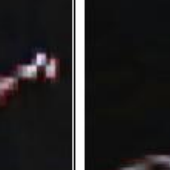

Property	B1	B2	B3	B4	B5	B6
Image format	PNG	PNG	PNG	PNG	PNG	PNG
Magnification (%)	312	308	309	308	311	305
Size(Kilobyte)	181	186	181	182	182	186
Frame (cm)	15.67 X 15.45	15.81 X 15.67	15.45 X 15.59	15.52 X 15.67	15.67 X 15.52	15.67 X 15.81
Frame(pixel)	217 X 214	218 X 217	214 X 216	215 X 217	217 X 215	217 X 219
Original image						
Analyzed image						

Table 4. Image analysis and properties of track like cosmic hits

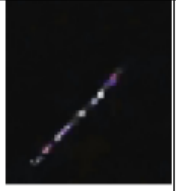

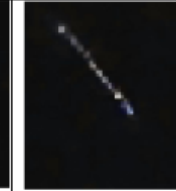

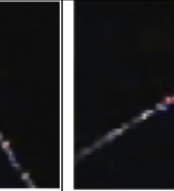





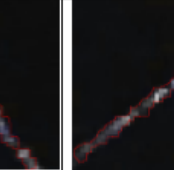
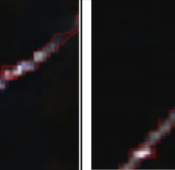
Property	C1	C2	C3	C4	C5	C6
Image format	PNG	PNG	PNG	PNG	PNG	PNG
Magnification (%)	310	307	305	304	310	306
Size(Kilobyte)	184	186	187	187	184	184
Frame (cm)	15.74 X 15.59	15.74 X 15.74	15.81 X 15.81	15.74 X 15.59	15.74 X 15.59	15.59 X 15.74
Frame(pixel)	218 X 219	218 X 218	219 X 219	218 X 220	218 X 216	216 X 218
Original image						
Analyzed image						

Table 5. Image analysis and properties of deblending and join track cosmic hits

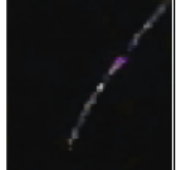
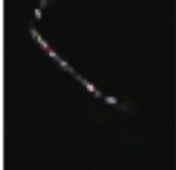
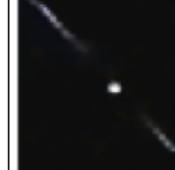
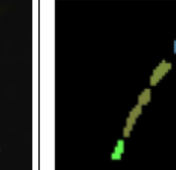

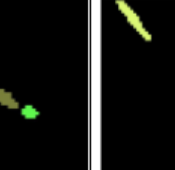


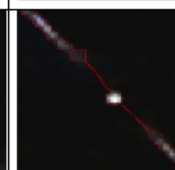

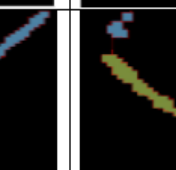
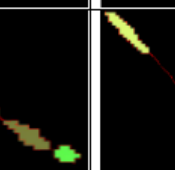
Property	D1	D2	D3	D4	D5	D6
Image format	PNG	PNG	PNG	PNG	PNG	PNG
Magnification (%)	308	308	309	324	329	326
Size(Kilobyte)	182	184	181	175	171	173
Frame (cm)	15.52 X 15.67	15.67 X 15.67	15.52 X 15.59	15.67 X 14.87	15.59 X 14.66	15.59 X 14.80
Frame(pixel)	215 X 217	217 X 217	215 X 216	217 X 206	216 X 203	216 X 205
Original image						
Analyzed image						

Table 6. Selected descriptive statistics of captured (CCD and CMOS) cosmic hits evaluated by image the analyzer.

Cosmic hit Category	Image ID	Actual Area(cm ²)	Actual Perimeter (cm)	Actual X length(cm)	Actual y length(cm)	Actual Circularity (cm)
Spot-like hits: ellipticity near 1, solidity near 1	A1	4.6412 ± 0.0822	9.2445 ± 0.1969	8.5351 ± 0.0160	7.1868 ± 0.0148	0.6830 ± 0.0264
	A2	0.3503 ± 0.0228	2.3681 ± 0.0791	8.0211 ± 0.0161	7.8045 ± 0.0161	0.7852 ± 0.0016
	A3	2.1329 ± 0.0646	7.5809 ± 0.1526	8.2551 ± 0.0116	7.0782 ± 0.0241	0.4667 ± 0.0183
	A4	3.5977 ± 0.0994	8.5771 ± 0.0914	8.0129 ± 0.0382	7.1874 ± 0.0139	0.6147 ± 0.0223
	A5	2.7053 ± 0.0766	7.5767 ± 0.1714	7.6146 ± 0.0283	6.9126 ± 0.0216	0.5926 ± 0.0219
	A6	3.0295 ± 0.1544	9.1635 ± 0.3944	8.2647 ± 0.0723	7.4028 ± 0.0197	0.4539 ± 0.0194
Worm-like hits: ellipticity ~0.5, solidity < 0.7,	B1	6.8450 ± 0.3236	2.6668 ± 0.0354	8.3753 ± 0.0315	4.0092 ± 0.0694	0.1211 ± 0.0079
	B2	6.1601 ± 0.2428	22.0068 ± 0.5922	6.7158 ± 0.0598	6.9661 ± 0.0104	0.1599 ± 0.0049
	B3	6.4760 ± 0.1509	23.1692 ± 0.2430	6.5973 ± 0.0217	6.6419 ± 0.0975	0.1517 ± 0.0053
	B4	7.1140 ± 0.2125	27.9080 ± 0.4149	8.7805 ± 0.1368	6.5411 ± 0.0149	0.1148 ± 0.0030
	B5	12.3276 ± 0.9998	50.0366 ± 0.4934	6.6299 ± 0.0628	6.0234 ± 0.3023	0.0617 ± 0.0040
	B6	8.1273 ± 0.1767	33.1562 ± 0.7916	5.7663 ± 0.1337	6.1957 ± 0.1271	0.0931 ± 0.0061
Track-like hits: ellipticity > 0.6, solidity > 0.7	C1	7.0984 ± 0.3353	28.3886 ± 0.6394	5.7815 ± 0.0375	5.1884 ± 0.0468	0.1106 ± 0.0029
	C2	7.0890 ± 0.5203	26.8192 ± 0.5222	5.9916 ± 0.0592	5.9916 ± 0.0592	0.1242 ± 0.0133
	C3	5.9354 ± 0.6097	25.8268 ± 1.7779	6.0966 ± 0.0637	10.0372 ± 0.0583	0.1260 ± 0.0192
	C4	7.5748 ± 0.4807	30.9946 ± 0.6458	9.6129 ± 0.0526	5.3909 ± 0.0550	0.0990 ± 0.0031
	C5	9.2042 ± 0.4493	35.9966 ± 0.9134	5.8541 ± 0.0772	6.2991 ± 0.0450	0.0893 ± 0.0036
	C6	10.0684 ± 0.2829	38.2832 ± 0.2110	7.5897 ± 0.0421	6.4443 ± 0.0893	0.0864 ± 0.0032
Deblending and join track from the same hit	D1	10.1276 ± 0.6454	40.2278 ± 0.7700	9.0531 ± 0.0215	9.0846 ± 0.0535	0.0788 ± 0.0064
	D2	8.2658 ± 1.0509	3.4478 ± 0.1302	5.4263 ± 0.0560	10.2744 ± 0.0697	0.0880 ± 0.0148
	D3	8.1127 ± 0.3538	44.3098 ± 0.4947	6.5995 ± 0.0486	9.2054 ± 0.0566	0.0520 ± 0.0032
	D4	9.6097 ± 0.1426	38.9676 ± 0.8872	8.9795 ± 0.0846	8.2020 ± 0.1167	0.0796 ± 0.0044
	D5	7.8948 ± 0.5315	35.0112 ± 0.2724	5.6897 ± 0.0203	9.0064 ± 0.0552	0.0810 ± 0.0068
	D6	6.5542 ± 0.4201	41.1512 ± 0.4028	6.6300 ± 0.0418	8.6597 ± 0.0377	0.0486 ± 0.0022

Table 1 is the image analysis parameters that were employed in characterizing the CCD/CMOS images. The defined distance in pixels covers the entire area surface of all the generated images per unit centimeter. Tables 2, 3, 4, and 5 disclose the analyzed images with image j software with the identified spot like (A), wormlike (B), a track like (C), and deblending/joint track (D) cosmic hits. Each result estimated specified characteristics in terms of the format, magnification, size, and frames of the processed images. Obviously, with their original smaller sizes, the proposed level of magnifications enhanced the application of the software in the resolutions and calculations of their properties. In table 6, five runs or determinations were engaged for the final statistical evaluations of their actual surface areas, perimeters, x/y lengths, and circularity which are the measures of roundness. The computed values were statistically generated by the combination of the respective mean values with the standard deviations. Therefore, the actual properties of the categorized cosmic hits via the CCD/CMOS sensors with respect to the defined parameters can be deduced from Table 6.

4.0 CONCLUSION

These outcomes with the cosmic-ray hits as images can be referenced in future analysis with respect to energies, frequencies, and other factors that characterized this radiation perhaps at different systems. Hence, a clearer understanding of these natural phenomena should begin to be unlocked as all the hits with high energy characteristics

were successfully analyzed with precise statistical results. In other words, the limitation observed with the smaller coverage devices especially with the smartphone of 1mm² area detection and the approach with cosmic watch [21] have been significantly addressed image J particle analyzer from the dark-framed and background cosmic hits.

5.0 REFERENCES

1. Astrophysics. THE SEDONA EFFECT. (2020). <https://www.sedonanomalies.com/astrophysics.html>.
2. Cosmic Rays. Hyperphysics.phy-astr.gsu.edu. (2020). <http://hyperphysics.phy-astr.gsu.edu/hbase/Astro/cosmic.html>.
3. Tietz & Rarr, V. (2020). Victor Franz Hess and the Cosmic Radiation. SciHi Blog. <http://scihi.org/victor-franz-hess-cosmic-radiation/>.
4. PANDEY, P. (2014). MYSTERY OF PHYSICS PROBLEMS. Physicsitarsi1.blogspot.com. <https://physicsitarsi1.blogspot.com/2014/07/>.
5. Cosmic ray - Info galactic: the planetary knowledge core. Infogalactic.com. (2020). https://infogalactic.com/info/Cosmic_ray.
6. Coursehero.com. (2020). <https://www.coursehero.com/file/74467555/Cosmic-raydocx/>.

7. Nick Connor (2019). What is Cosmic Radiation - Cosmic Ray – Definition. Radiation Dosimetry. <https://www.radiation-dosimetry.org/what-is-cosmic-radiation-cosmic-ray-definition/>.
8. Ray, C. (2020). Cosmic ray. Amedleyofpotpourri.blogspot.com. <https://amedleyofpotpourri.blogspot.com/2015/01/cosmic-ray.html>.
9. Nagar, G. (2015). COSMICRAYS. Cosmicraysghs78.blogspot.com. <https://cosmicraysghs78.blogspot.com/>.
10. User, S. (2020). Branches of astronomy. Mindmapcharts.com. <http://mindmapcharts.com/index.php/gk/astronomy/72-branches-of-astronomy>.
11. Gupta, S. (2020). London Journals Press - Cosmic Ray Origins: Part 1. Frequency Upshifting of light Rays / Electromagnetic Radiation near stars in Dynamic Universe Model. <https://journalspress.com/cosmic-ray-origins-part-1-frequency-upshifting-of-light-rays-electromagnetic-radiation-near-stars-in-dynamic-universe-model>.
12. Cosmic ray. En.wikipedia.org. (2020). https://en.wikipedia.org/wiki/Cosmic_ray.
13. Michal Niedzwiecki et al (2019). Recognition and classification of the cosmic-ray events in images captured by CMOS/CCD cameras. (2020). https://www.researchgate.net/publication/335617672_Recognition_and_classification_of_the_cosmic-ray_events_in_images_captured_by_CMOSCCD_cameras.
14. Tedpella.com. (2020). Background Information on CCD and CMOS Technology https://www.tedpella.com/cameras_html/ccd_cmos.htm.
15. Teledynedalsa.com. (2020) .CCD vs. CMOS | Teledyne DALSA. (2020). <http://www.teledynedalsa.com/en/learn/knowledge-center/ccd-vs-cmos/>.
16. CMS Collaboration, Measurement of the charge ratio of atmospheric muons with the CMS detector, Phys.Lett.B692:83-104,2010 [arXiv:1005.5332]
17. Zheng, C. X. et al (2015). An improved method for object detection in astronomical images, MNRAS 451 (4):4445-4459. 2015. [doi:10.1093/mnras/stv1237]
18. M. Fisher-Levine and A. Nomerotski (2015). Characterizing CCDs with cosmic rays, JINST [doi:10.1088/1748-0221/10/08/c08006]
19. Matthew Meehan et al. (2017). The particle detector in your pocket: The Distributed Electronic Cosmic-ray Observatory, Instrumentation and Methods for Astrophysics ICRC 2017 [arXiv:1708.01281]
20. D. Heck and T. Pierog (2020). Extensive Air Shower Simulation with CORSIKA: A User's Guide, KIT - Universitat des Landes Baden-Württemberg und nationales Forschungszentrum in der Helmholtz-Gemeinschaft, <https://web.ikp.kit.edu/corsika/usersguide/usersguide.pdf>
21. The Cosmic Watch project [http://www.cosmicwatch.lns.mit.edu/]